

A LOW POWER, HIGH GAIN, LOW NOISE AMPLIFIER WITH IMPROVED NOISE FIGURE AND INPUT MATCHING FOR ULTRA WIDE BAND APPLICATIONS*

V. VAITHIANATHAN^{1**}, J. RAJA² AND R. SRINIVASAN³

¹Department of ECE, SSN College of Engineering, Kalavakkam, Chennai, India – 603110
Email: vaithianathanv@ssn.edu.in

²Department of ECE, Sri Sairam Engineering College, Tambaram, Chennai, India – 600044

³Department of IT, SSN College of Engineering, Kalavakkam, Chennai, India – 603110

Abstract– In this paper, two low noise amplifiers (LNAs), one without feedback and another one with active shunt partial feedback, are proposed for ultra wide band (UWB) applications. Both the proposed LNAs are designed using 90 nm CMOS technology and their performance parameters are analyzed by using post layout simulation. The proposed LNA without feedback achieves a power gain (S_{21}) of 16.4 dB over the band of 3 – 10.4 GHz with NF (Noise Figure) in the range of 4.9 – 5.2 dB. This high NF has been reduced to 2.4 – 2.7 dB by employing active shunt partial feedback. The proposed LNA with active shunt partial feedback achieves a power gain of 15 dB over the band of 2 – 12 GHz. The input matching (S_{11}) and output matching (S_{22}) are less than – 10 dB while maintaining the reverse isolation (S_{12}) is less than -60 dB for both of the proposed circuits. Both circuits, with and without active shunt partial feedback, maintain better linearity with in-band third order input intercept point (IIP₃) of – 1 dBm and – 4.242 dBm, respectively and consume 3.643 mW and 2.862 mW of power while operating at 1 V power supply.

Keywords– Active-shunt partial feedback, noise figure, input matching, shunt-series peaking, current-reuse, third order input intercept point

1. INTRODUCTION

In recent years, both the academia and industry have shown interest in UWB technology as it offers a promising solution to the radio frequency (RF) spectrum scarcity by allowing new services to co-exist with other radio systems with minimal or no interference [1]. UWB technology is suitable for short range and high data rate wireless applications which include cognitive radio, ground penetrating radars, imaging and surveillance systems, safety/health monitoring, wireless home video links, etc.

In February 2002, the Federal Communication Committee (FCC) approved the first report and order for commercial use of UWB technology under strict power emission limits for various devices. The UWB signals should have an average power spectral density limit of –41 dBm/MHz in the frequency range of 3.1 – 10.6 GHz. As defined by the FCC, UWB signals must have bandwidth of more than 500 MHz or fractional bandwidth larger than 20 percent at every point of transmission. The fractional bandwidth [1] is defined as the ratio of bandwidth to center frequency as given in Eq. (1).

$$B_f = \frac{BW}{f_{center}} 100\% = \frac{f_h - f_l}{[f_h + f_l]/2} 100\% \quad (1)$$

where f_h and f_l are the highest and lowest cutoff frequencies of the UWB spectrum respectively.

*Received by the editors December 19, 2011; Accepted December 17, 2012.

**Corresponding author

There are two types of UWB communication systems based on (i) direct sequence code division multiple access (DS-CDMA) approach and (ii) multi-band orthogonal frequency division multiplexing (MB-OFDM) approach [2]. The DS-UWB is a single-band approach and is fundamentally different from all other communication techniques because it employs extremely narrow RF pulses to communicate between transmitters and receivers. The usage of short-duration pulses helps in achieving a very wide bandwidth and offers several advantages, such as high throughput, robustness to jamming and coexistence with current radio services. As shown in Fig. 1, the entire UWB spectrum is divided into two bands, namely lower and upper bands. The lower band occupies the spectrum in the range of 3.1 GHz to 4.85 GHz, while the upper band lies in the range of 6.2 GHz to 9.7 GHz. The DS-CDMA approach, also called impulse radio, provides data rates from 28 to 1320 Mb/s within the transmission bands from 3.1 to 4.85 GHz and from 6.2 to 9.7 GHz [2]. In the MB-OFDM approach [3], the entire UWB spectrum is divided into 14 bands, where each band has a bandwidth of at least 500 MHz. The MB-OFDM approach is planned into six groups as illustrated in Fig. 1 and the operation within the first group is mandatory, while all the other groups are optional.

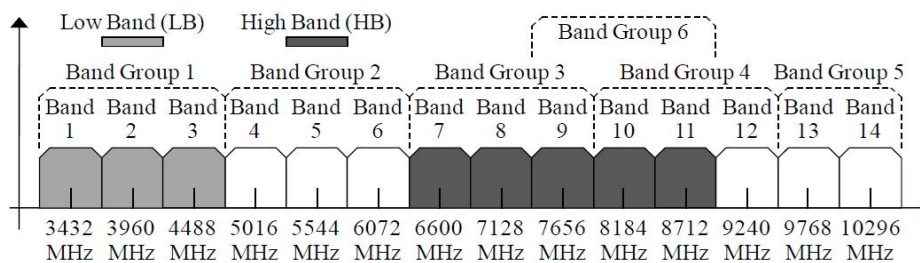


Fig. 1. UWB Standards [3]

The received UWB signal exhibits very low power-spectral density (PSD) at the receiving antenna due to the stringent power-emission limitation set by FCC at the transmitting antenna and the transmission path loss introduced in the channel. The received signal power is typically three orders of magnitude smaller than that of the narrow-band transmission systems [2]. The low power reception makes the realization of front-end circuits of the UWB receiver very difficult. The LNA becomes an important component in the front-end circuits since the LNA decides the overall receiver sensitivity.

The main purpose of the LNA is to amplify the weak signal received from the antenna to an acceptable level while trying to reduce the additional self generated noise. The main design requirement for the UWB LNA is to provide sufficient gain over the entire 7.5 GHz bandwidth. A wide-band input matching of 50 Ω , a low NF and very low power consumption are required to enhance the sensitivity of UWB receiver [2]. The linearity of an amplifier is described in terms of 1dB compression point (P_{1dB}) and third-order input intercept point (IIP_3). Thus, the LNA design remains the biggest challenge in the implementation of a UWB system.

The LNA can be designed in different topologies such as distributed amplifier, common gate (CG), common source (CS), differential amplifier and resistive shunt feedback amplifier [4]. Most of the recent work done on the LNA are focused on achieving an optimal trade-off between the LNA parameters by using these different amplifier. The distributed amplifier [5] was capable of providing a very large bandwidth because of its unique gain-bandwidth trade-off. However, high power consumption and large chip area made this topology unsuitable for typical low-power and low-cost UWB applications. The CG amplifier [6] achieved excellent wideband input matching and better input-output isolation but it suffered from high NF and low power gain. The inductive source degeneration amplifier [7] provided wide bandwidth, high power gain and low NF. The inductive source degeneration amplifier used filter network for obtaining better input matching. This filter network occupied large chip area and the insertion loss of

the filter network caused the NF of the LNA to degrade rapidly with frequency. Differential LNA [8] provided high power gain, high linearity and low NF, but it suffered from high power consumption and large chip area. The inductive degenerated LNA [9] achieved a very low NF with good input and output impedance matching by using reactive feedback and coupled inductors, but it suffered from high power consumption.

The resistive feedback LNA [10] used a cascode amplifier as the core stage with current reuse structure for input matching and filter network for output matching. The proposed circuit in [10] had problems of poor input and output matching with high power consumption. The wideband resistive feedback CMOS LNA [11] with a noise cancellation technique provided very low NF but it supported only the lower band of UWB. Meamar [12] proposed a wideband CMOS LNA by employing the concept of mutual coupling technique implemented using a symmetric center-tap inductor. A frequency widening network was designed with a center-tap inductor at the input and the output of an LNA to achieve bandwidth extension with a single stage amplifier and this LNA consumed very low power but its bandwidth was only 3 – 8 GHz. A wideband resistive feedback CMOS LNA with a noise cancellation technique proposed in [13] achieved very good power gain only for the lower part of the UWB and consumed high power. Ruey-Lue Wang [14] proposed a cascode LNA with an additional voltage current feedback to operate over the full-band of UWB spectrum. This circuit topology achieved a wideband input matching with the help of a multi-section LC resonant configuration. Even though it provided very good linearity, it suffered from very high power consumption.

From the survey of recent works on resistive shunt feedback LNAs, it is understood that the resistive shunt feedback topology did not provide high gain and low NF simultaneously while satisfying wideband input matching and flat gain requirements. So, it is required to have a low power LNA which provides high gain with good uniformity, low NF and better linearity simultaneously. Our work addresses these issues with the help of active shunt partial feedback employed in the current reuse cascode LNA. Section 2 discusses the operation of both the proposed LNAs with their equivalent circuits and design equations. Section 3 illustrates the post layout simulation results and analysis. The results are compared with recently reported resistive shunt feedback LNAs. Section 4 concludes the paper.

2. PROPOSED LOW NOISE AMPLIFIERS

This paper presents an LNA with cascode amplifier as a core stage, a simple pi (π) network to obtain wideband input matching and a current reuse network to achieve low power operation. But this LNA suffers from very high NF. An active shunt partial feedback is employed in the core stage to improve the noise performance and linearity without affecting other parameters. A variety of bandwidth enhancement techniques [4] such as series peaking, shunt peaking, shunt-series, T-coil and f_T doublers using Darlington pairs were presented in the literature. In this work, shunt-series peaking is used for bandwidth enhancement in both the proposed LNAs.

The proposed LNA without feedback and its equivalent circuit are shown in Figs. 2 and 3 respectively. The transistors M_1 (common source) and M_2 (common gate) form the cascode amplifier. The use of cascode amplifier eliminates Miller effect and provides better isolation from the output signal. The current re-use network is formed by the inductors L_3 , L_4 and the capacitor C_2 . A portion of the supply voltage is dropped across capacitor C_2 which is used to bias the upper transistor and therefore it derives less current from the power supply. At higher frequencies, a low impedance path is created through L_4 and C_2 as the impedance of L_3 becomes large. As a result, the input signal can be amplified twice with this structure. Thus the current-reuse technique increases the gain while consuming much less power. Shunt-series peaking network constructed with the help of R_1 , L_5 and L_6 , is used to extend the bandwidth.

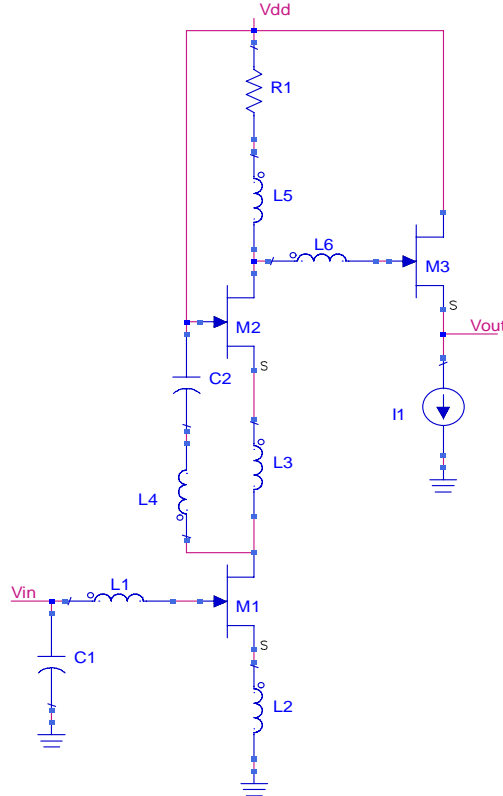


Fig. 2. Proposed LNA without feedback

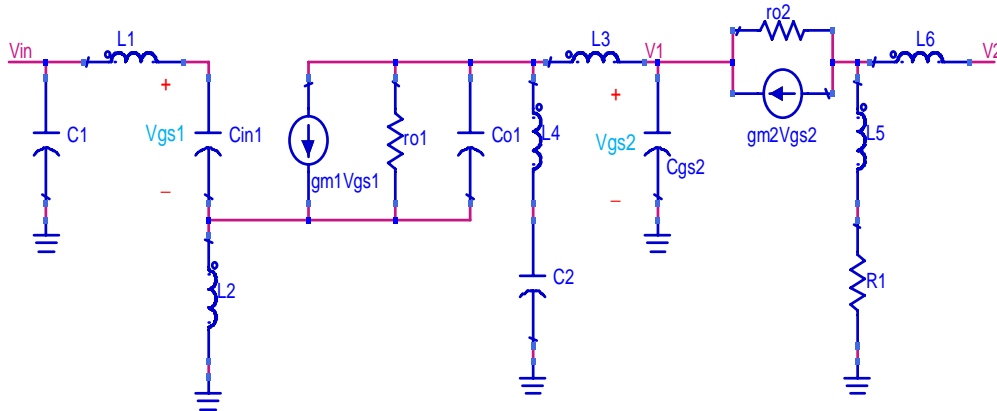


Fig. 3. Equivalent Circuit for core stage of the LNA proposed in Fig. 2

The input matching is achieved using the pi (π) network formed at the input by the capacitor C_1 and the inductors L_1 and L_2 . The input capacitance (C_{in1}) of M_1 makes the input impedance seen at the gate of M_1 to be purely reactive, thereby providing a wideband input matching. The input impedance is given by the Eq. (2).

$$Z_{in} \approx \left(\frac{1}{sC_1} \right) \parallel \left(sL_1 + \frac{1}{sC_{in1}} + \left(1 + g_{m1} \left(sL_1 + \frac{1}{sC_{in1}} \right) \right) sL_2 \right) \quad (2)$$

The capacitance C_{in1} that represents the parallel combination of the gate-to-source capacitance (C_{gs1}) and the equivalent drain-to-gate Miller Capacitance (C_{gd1}) of M_1 , is given by the Eq. (3).

$$C_{in1} \approx (1 + A_{V1})C_{gd1} + C_{gs1} \quad (3)$$

The gain of the common source amplifier (M_1) is given by the Eq. (4).

$$A_{V1} \approx \frac{-g_{m1}Z_{L1}}{1 - g_{m1}Z_{L1}(sL_2)} \quad (4)$$

where

$$Z_{L1} \approx r_{o1} \parallel \left(sL_4 + \frac{1}{sC_2} \right) \left(sL_3 \parallel \frac{1}{sC_{gs2}} \right) \quad (5)$$

The inductor L_2 acts as a negative feedback (source degeneration) thereby stabilizing the gain of the CS amplifier. The overall gain of the proposed LNA without feedback is derived as in Eq. (6).

$$A_{VTotal} \approx A_{V1} \times A_{V2} \times A_{V3} \quad (6)$$

Here, A_{V1} is the gain contributed by the transistor (M_1) and is given in Eq. (4). The gain A_{V2} , contributed by the transistor (M_2), is derived as in Eq. (7).

$$A_{V2} \approx g_{m2}Z_{L2} \quad (7)$$

where

$$Z_{L2} \approx r_{o2} \parallel \left(sL_5 + R_1 \right) \left(sL_6 \parallel \frac{1}{sC_{gs3}} \right) \quad (8)$$

The gain A_{V3} , contributed by the transistor (M_3), is given in Eq. (9).

$$A_{V3} \approx \frac{g_{m3}r_{o3}}{1 + g_{m3}r_{o3}} \quad (9)$$

The common drain amplifier has low output impedance thereby enabling easy output matching of 50 Ω . The output impedance can be easily matched by using the Eq. (10).

$$Z_{out} \approx r_{o3} \parallel \frac{1}{g_{m3}} \quad (10)$$

The common drain amplifier is a source follower with a transistor and a current source. A constant current source is provided for two purposes. It acts as the load and also helps to maintain common drain amplifier in saturation. Thus, the circuit is biased by exact selection of component values and transistor dimensions.

Siroos Toofan [15] demonstrated an improved noise modeling concept and derived the equation for NF of the inductive source degenerated common source amplifier. Since the input stage of our proposed circuit is also an inductive source degenerated common source amplifier, the same procedure is adopted in our design. The NF of the LNA without feedback is given in Eq. (11).

$$NF \approx 1 + \frac{R_g + R_{L1}}{R_s} + \frac{\gamma\chi}{\alpha Q_{in}} \left(\frac{\omega_0}{\omega_T} \right) \left(\frac{R_s + R_{L1} + R_{nqs} + R_g}{R_s} \right) \quad (11)$$

where

$$\chi = 1 + \frac{\delta\alpha^2}{5\gamma} (1 + Q_{in}^2) + 2|C| \sqrt{\frac{\delta\alpha^2}{5\gamma} (1 + Q_{in}^2)} \quad (12)$$

$$Q_{in} = \frac{1}{[(R_s + R_{L1} + R_{nqs} + R_g)C_{in1}\omega_0]} \quad (13)$$

The parameters γ , δ , α are foundry dependent parameters and are taken from 90nm CMOS BSIM 4.5 transistor model for our design.

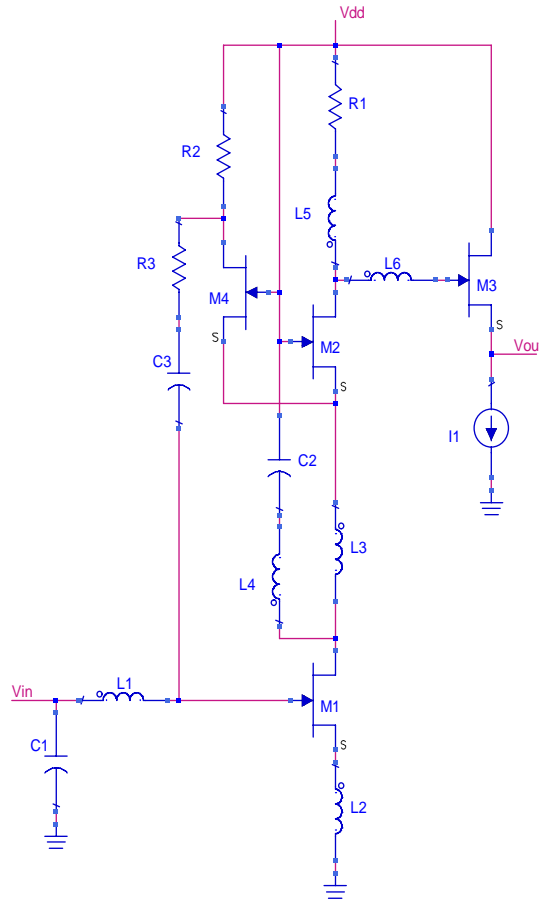


Fig. 4. Proposed LNA with active shunt partial feedback

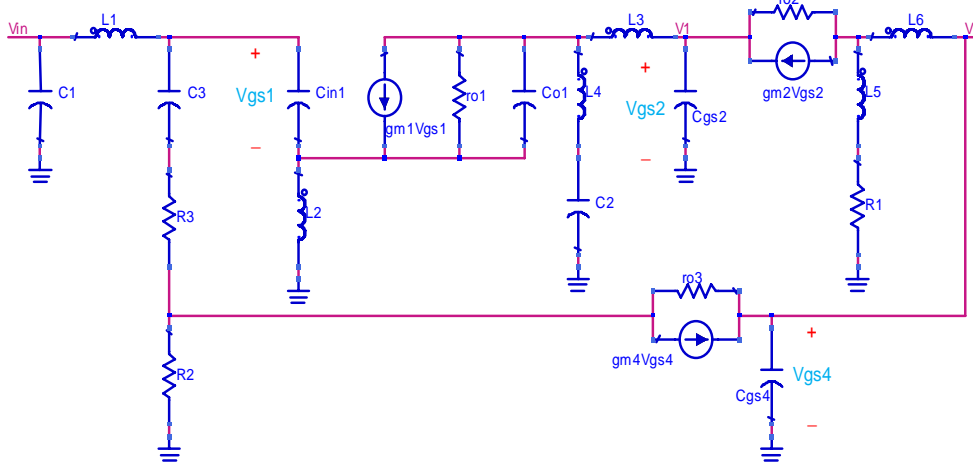


Fig. 5. Equivalent Circuit for the core stage with active shunt partial feedback of LNA proposed in Fig. 4

The noise performance of the first LNA is not optimum where as all other parameters are at acceptable levels. An active shunt feedback is introduced in the second circuit as shown in Fig. 4 to improve the NF along with input matching. Its equivalent circuit for the core stage is presented in Fig. 5. The active shunt-shunt feedback can be considered to be made up of two loops viz. the open loop and the closed loop. The open loop is formed by M₁ and M₂ and it provides very good amplification along with good output matching by using current reuse technique. The closed loop of the active shunt feedback is formed by M₄, R₂, R₃ and C₃.

The closed loop helps in achieving very good input matching and better NF while reducing the signal distortion at the output. The loop gain β is given by the Eq. (14).

$$\beta \approx g_{m1} \frac{\frac{1}{\frac{1}{g_{m2}} + \frac{1}{g_{m4}}}}{R_2} \approx g_{m1} \frac{W_2}{W_2 + W_4} R_2 \quad (14)$$

where g_{m1} is the transconductance of the transistor M_1 , W_2 is width of the transistor M_2 , W_4 is width of the transistor M_4 and R_2 is the load resistance of the feedback loop. The input impedance with active shunt feedback (Z_{If1}) is given by Eq. (15).

$$Z_{If1} \approx \left(\frac{Z_{in}}{1 + \beta Z_{in}} \right) \quad (15)$$

The impedance (Z_{L1}) at the source of M_2 provides a path for the noise current $I_{nd,M4}$ of the cascode transistor M_4 . Since the gate bias voltage is the same for both M_2 and M_4 , the noise current $I_{on,M4}$ flows from M_4 to the output at the ratio between the source impedance of M_2 and M_4 . The noise current $I_{on,M4}$ is given by the Eq. (16).

$$I_{on,M4} \approx I_{nd,M4} \frac{\frac{1}{\frac{1}{g_{m4}} + \frac{1}{g_{m2}}}}{W_4 + W_2} \approx I_{nd,M4} \frac{W_4}{W_4 + W_2} \quad (16)$$

where g_{m2} and g_{m4} are the transconductances of the transistors M_2 and M_4 respectively. The application of the active shunt partial feedback reduces the gain contributed by M_1 and is given by the Eq. (17).

$$A_{V1,fb} \approx \left(\frac{A_{V1}}{1 + \beta A_{V1}} \right) \quad (17)$$

From the Eqs. (14) and (16), it is evident that the value of W_2 should be as high as possible to achieve the better input matching and to reduce the output noise. But the Eqs. (14) and (17) show that high value of W_2 reduces the gain contributed by the transistor M_1 . So, it is necessary to choose the values of W_2 and R_2 very carefully. In the proposed design, the ratio (W_2/W_4) is chosen to be 10:1 to achieve better input matching and low NF with acceptable power gain.

3. SIMULATION RESULTS

The proposed LNAs are designed using 90 nm CMOS technology and the post layout simulations are performed. The values of the power gain (S_{21}), noise figure (NFmin), input matching (S_{11}), output matching (S_{22}) and reverse isolation (S_{12}) are plotted in dB (y-axis) versus the frequency range of 2 – 12 GHz (x-axis) in Figs. 6-10. The values of stability factor (K) and Delta (Δ) are presented in Figs. 11–14 over the band of interest. The linearity analysis of the proposed LNAs are given in terms of IIP₃ by plotting input power (Pin in dBm) versus output power (Pout in dBm) in Figs. 15 and 16. The summary of the simulation results of the proposed LNAs and quantitative comparison with recently reported resistive shunt feedback LNAs are presented in Table 1 at the end of this section.

The power gain (S_{21}) varies from 16.4 dB to 19.4 dB over the band of 3.1GHz – 10.4 GHz for the circuit without feedback. With the help of active shunt partial feedback, the gain variation is minimized and it varies from 15 dB to 16.6 dB over the band of 2 GHz – 12 GHz. From the Fig. 6, it is evident that the proposed active shunt partial feedback ensures the gain uniformity with 0.6 dB variation in the UWB frequency band of 3.1 GHz to 10.6 GHz.

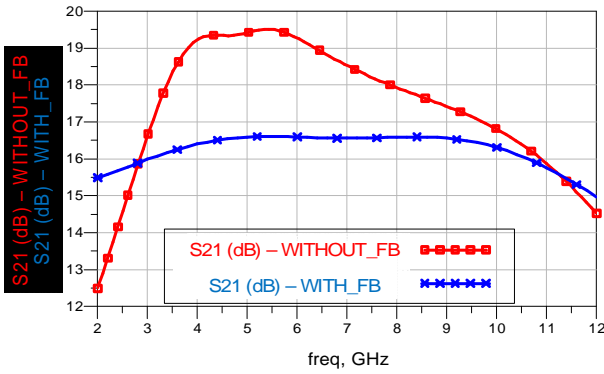


Fig. 6. Power gain (S_{21})

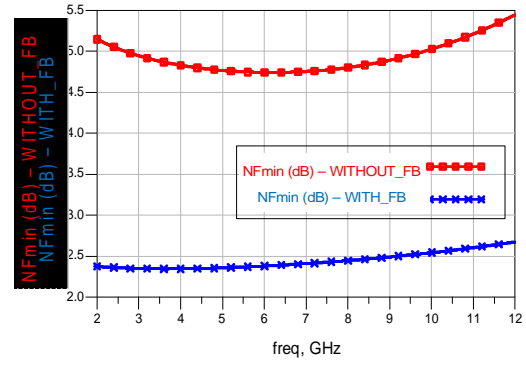


Fig. 7. Noise figure (NF)

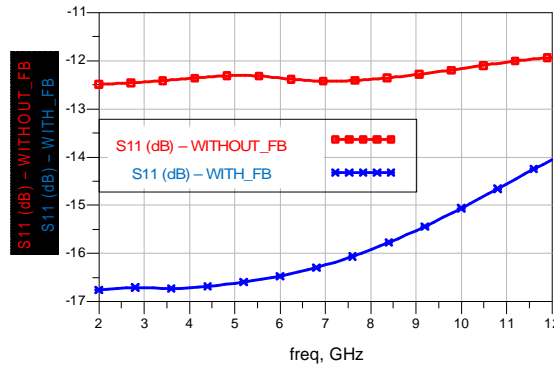


Fig. 8. Input matching (S_{11})

In the LNA without feedback, the achieved NF falls in the range of 4.9 dB to 5.3 dB over the band of 3.1GHz – 10.4GHz. From Fig. 7, it is evident that the use of an active shunt partial feedback ensures an improved noise performance as the NF falls in the range of 2.4 dB to 2.7 dB over the band of 2 GHz – 12 GHz. This is a highly remarkable improvement obtained by the proposed active shunt partial feedback circuit. For the circuit without feedback that uses pi-filter and inductive source degeneration, the input matching falls below -12.2 dB over the band of 3.1 GHz to 10.4 GHz, as shown in Fig. 8. The active shunt partial feedback technique has helped in achieving a better input matching of -14 dB over the band of 2 GHz – 12 GHz. This response further justifies the use of the active shunt partial feedback for improving input matching along with NF.

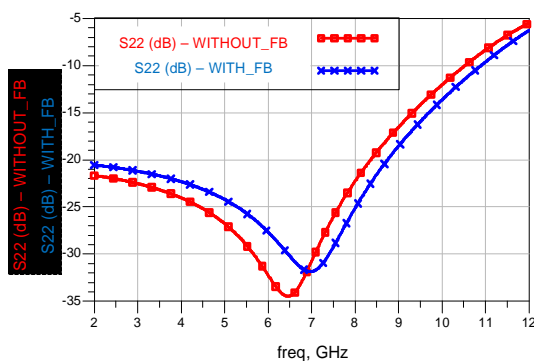


Fig. 9. Output matching (S_{22})

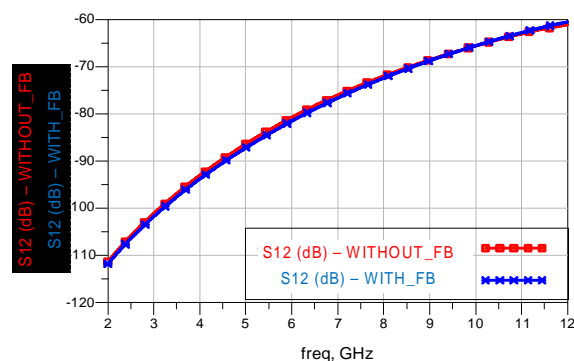


Fig. 10. Reverse isolation (S_{12})

Figure 9 shows the output matching characteristics. It is found that a very good output impedance matching is achieved with the minimum value of -34 dB at 6.5 GHz and less than -10 dB over the entire band of 3.1GHz to 10.4 GHz for the circuit without feedback. Thus, the application of active shunt partial feedback helps to achieve the output matching in the range of -10 to -20 dB over the band of 2 GHz to

11 GHz with a minimum value of -32 dB at 7 GHz. The reverse isolation characteristic is shown in Fig. 10, and it is found that the minimum value is about -112 dB. The reverse isolation is found to be well below -60 dB throughout the entire frequency range of 2 GHz – 12 GHz, thereby offering better stability.

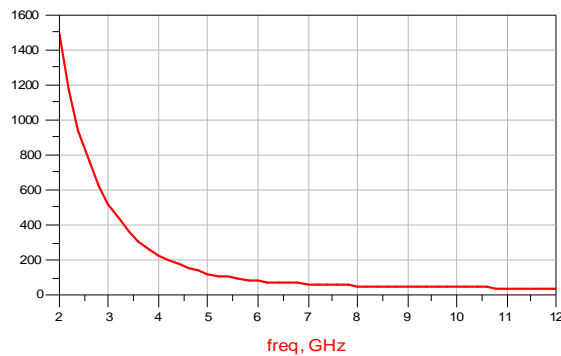


Fig. 11. Stability factor (K) for the LNA without feedback

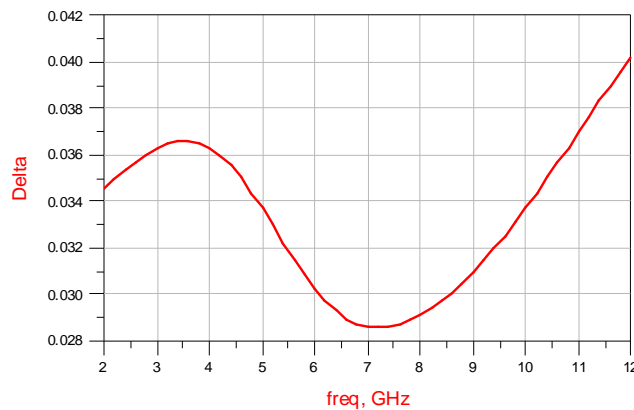


Fig. 12. Delta (Δ) for the LNA without feedback

The stability [16] of the proposed amplifier is determined by using Rollet’s Stability Factor (K) [17] from the set of S parameters at the frequency of operation by using the Eqs. (18) and (19). The values of these two stability parameters K and Δ help to determine whether the amplifier is stable or not.

$$K = \frac{1 - |S_{11}|^2 - |S_{22}|^2 + |\Delta|^2}{2|S_{21}S_{12}|} \tag{18}$$

where

$$|\Delta| = |S_{11}S_{22} - S_{12}S_{21}| \tag{19}$$

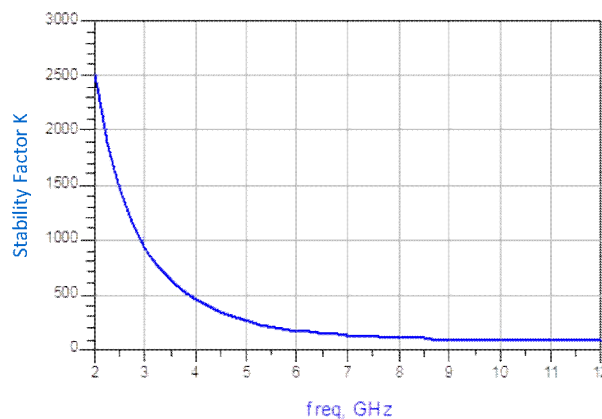


Fig. 13. Stability factor (K) for the LNA with active shunt partial feedback

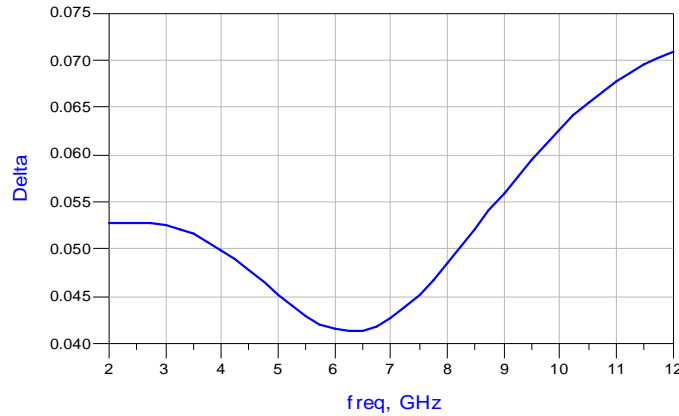


Fig. 14. Delta (Δ) for the LNA with active shunt partial feedback

The parameters must satisfy $K > 1$ and $|\Delta| < 1$ for a transistor to be unconditionally stable. It is evident from Figs. 11 to 14 that both the proposed circuits are unconditionally stable since the value of K is greater than 40 and the value of $|\Delta|$ is less than 0.071 for the entire band.

Linearity is the criterion that defines the upper limit of detectable RF input power and sets the dynamic range of the receiver. The linearity of an amplifier is described in terms of 1dB compression point (P_{1dB}) and third-order input intercept point (IIP_3). The 1dB compression point is defined as the input level at which the gain drops by 1dB due to the saturation effect. As the low power UWB signal rarely suffers from gain compression, P_{1dB} is not calculated for UWB LNA [18]. A two tone test is used to measure the IIP_3 . The IIP_3 is calculated by applying two -20 dBm test tones separated by 2 MHz and swept from 2 – 12 GHz. From Fig. 15, it is observed that an IIP_3 of -4.242 dBm is achieved at 7 GHz for the proposed circuit without feedback. From Fig. 16, it is evident that the active shunt partial feedback employed in the proposed circuit helps us to achieve the linearity with an IIP_3 of -1 dBm at 7 GHz.

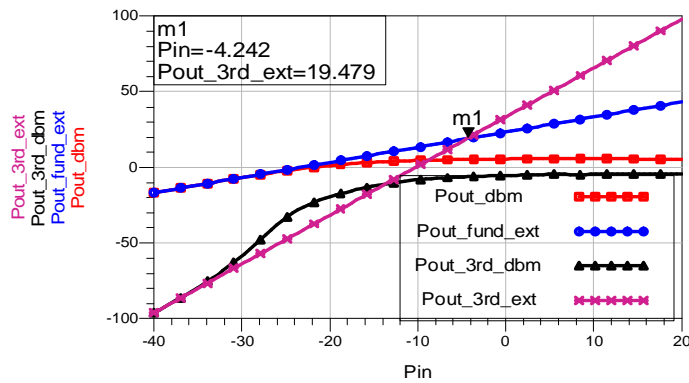


Fig. 15. Third order intercept point (IIP_3) with feedback

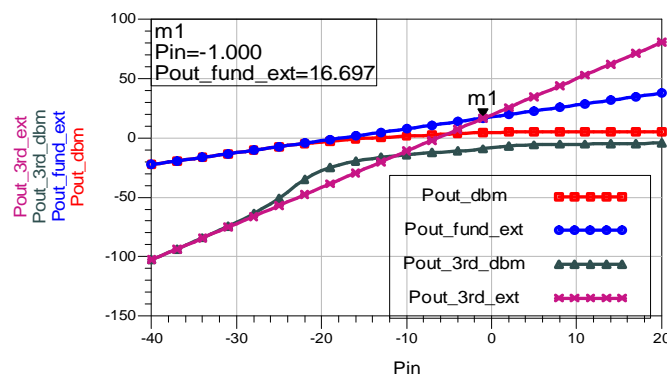


Fig. 16. Third Order Intercept Point (IIP_3) with active shunt partial feedback

Table 1. Simulation results summary and quantitative comparison with resistive feedback LNAs

Parameters	[9]	[10]	[11]	[12]	[13]	[14]	Our Work	
							Without FB	With FB
Technology	0.18 μ m CMOS	0.18 μ m CMOS	0.18 μ m CMOS	90 nm CMOS	90 nm CMOS			
Topology	Resistive Feedback	Resistive Feedback	Resistive Feedback	Cascode + Resistive Feedback	Resistive Feedback	Resistive Feedback	Cascode	Cascode + Active Shunt Partial Feedback
3dB Bandwidth (GHz)	4 – 10	3.1-10.6	3 – 5	3 – 8	0.7 – 6.5	3.1 – 10.6	3– 10.4	2 – 12
Power Gain S_{21} (dB)	12	9.7 \pm 1.1	6.82 – 9.51	15.2	12.5	7.4 – 9.2	16.4 -19.4	15 – 16.6
Noise Figure NF (dB)	0.2 – 0.8	3.4 – 3.84	3.26 – 4.16	3.14 – 6.8	3.5 – 4.2	4.1 – 7	4.9 – 5.2	2.4 – 2.7
Input Matching, S_{11} (dB)	< - 10	< - 6.7	<-11.8	- 8	< - 11	<-9.7	< -12.2	< - 14
Output Matching S_{22} (dB)	< - 10	< - 8.5	<-10.4	-	-	-	< - 10	< - 10
Reverse Isolation S_{12} (dB)	-	< -31	-	-	-	-	< - 60	<-60
IIP ₃ (dBm)	-	-3.5 @ 7 GHz	3.56 @ 4 GHz	- 6.63	- 5 @ 5 GHz	7.25 @ 6 GHz	- 4.242 @ 7 GHz	- 1 @ 7 GHz
Power Dissipation P_D (mW)	11.9	14.4	9.7 @ 1.8V	3.77 @ 1.8V	11.1 @ 1.8V	23.5 @ 1.0 V	2.862 @ 1V	3.643 @ 1V
FOM	17	-	-	-	7.5	-	10.87	24.22

The dc power consumption is calculated by measuring the total current drawn from 1 V power supply. The proposed LNA without feedback consumes 2.862 mW since it draws 2.862 mA from the power supply. The proposed LNA with active shunt partial feedback draws a slightly higher current of 3.643 mA leading to 3.643 mW of power consumption. A figure of merit (FOM) [5] suitable for evaluating the performance of a wideband LNA is given in Eq. (20).

$$FOM = \left[\frac{S_{21} \cdot BW(\text{GHz})}{(NF - 1) \cdot P_{dc}(\text{mW})} \right] \quad (20)$$

The proposed LNA without feedback achieves a FOM of 10.87, whereas the LNA with the active shunt partial feedback achieves a FOM of 24.22. The increase in FOM justifies the use of active shunt partial feedback for improving the performance.

4. CONCLUSION

In this work, the LNA with a cascode amplifier as the core stage is first designed with a simple pi-filter network to achieve wideband input matching and a voltage buffer to obtain broadband output matching. By employing the current reuse technique, a high gain of 19.4 dB is obtained over the entire UWB spectrum with low power consumption of 2.682 mW. The LNA achieves a FOM of 10.87 but it suffers with very high NF of 5.2 dB. The NF is reduced by using an active shunt partial feedback in the second circuit with wideband input matching and good linearity. Though there is a marginal increase in the power consumption of 3.643 mW, it achieves an improved FOM of 24.22 with very low NF of 2.4 dB over the band of 2 to 12 GHz. The active shunt partial feedback also helps to improve the IIP₃ from – 4.242 dBm to

– 1 dBm. Thus, the proposed LNA with active shunt partial feedback claims the advantages of flat gain over the band of interest, better input matching, very low NF, good linearity and low power consumption.

REFERENCES

1. Nekoogar, F. (2008). *Introduction to ultra wideband communications*. Chapter -1, pp. 1-44.
2. Wood, S. & Aiello, R. (2008). *Essentials of UWB*. Cambridge Univ. Press.
3. Lu, Y. & et al. (2006). A novel CMOS low-noise amplifier design for 3.1-to 10.6-GHz ultra-wide-band wireless receivers. *IEEE Transactions on Circuits and Systems – I: Regular Papers*, Vol. 53, No. 8, pp. 1683-1692.
4. Lee, T. H. (1998). *The design of CMOS radio-frequency integrated circuits*. 1st Ed. New York: Cambridge Univ. Press.
5. Del Pino, J., Diaz, R. & Khemchandani, S. L. (2010). Area reduction techniques for full integrated distributed amplifier. *AEU International Journal of Electronics Communications*, Vol. 64, Iss. 11, pp.1055-1062.
6. Chang, J. F. & Lin, Y. S. (2011). 0.99 mW 3-10 GHz common gate CMOS UWB LNA using T-match input network and self body bias technique. *Electronic Letters*, Vol. 47, Iss.11, pp. 658-659.
7. Zhang, H., Fan, X. & Sinencio, E. S. (2009). A low power linearized ultra wide band LNA design technique. *IEEE Journal of Solid-State Circuits*, Vol. 44, Iss. 2, pp. 320-330.
8. Hsu, H. M., et al. (2009). Noise analysis of inductive shunt series feedback technique used in ultra wide band low noise amplifier. *Proceedings of the Microwave Conference APMC*, pp. 1136-1139.
9. Salehi, M. R. et al. (2012). A 0.7 dB noise figure UWB CMOS LNA with reactive feedback in 0.18 μ m technology. *Proceedings of International Conference on Advances in Electrical and Electronics Engineering (ICAEE'2012)*, Penang, Malaysia pp. 349-352.
10. Chen, C. H. & Yang, J. R. (2010). The design a LNA of 3.1-10.6GHz UWB receive system. *Proceedings of Progress in Electromagnetic Research Symposium*, pp. 1534-1537.
11. Wang, W. et al. (2010). Design of low noise amplifier with shunt feedback for 3–5 GHz UWB receiver. *Proceedings of 12th IEEE International Conference on Communication Technology (ICCT)*, pp. 269-271.
12. Meamar, A., Chye, B. C., Anh, D. M. & Seng, Y. K. (2009). A 3–8 GHz low noise CMOS amplifier. *IEEE Microwave Wireless Components Letters*, Vol. 19, No. 4, pp. 254-247.
13. Hu, J., Zhu, Y. & Wu, H. (2008). An ultra-wideband resistive-feedback low-noise amplifier with noise cancellation in 0.18 μ m digital CMOS. *IEEE Topical Meeting on Silicon Monolithic Integrated Circuits in RF Systems (SiRF)*.
14. Wang, R. L. et al. (2007). A 1V full-band cascoded UWB LNA with resistive feedback. *Proceedings of IEEE International Workshop on Radio-Frequency Integration Technology*, pp. 188-190.
15. Toofan, S. et al. (2008). A 5.5-GHz 3mW LNA and inductive degenerative CMOS LNA noise figure calculation. *Proceedings of International Conference on Microelectronics*, pp. 1-5.
16. Azhari, S. J. & Shokoufia, M. (2011). New structure for current mode continuous time Gm-C filters. *Iranian Journal of Science and Technology, Transactions of Electrical Engineering*, Vol. 35, No. E1, pp. 25-43.
17. Krstic, D. V. (2007). Linvill and Rollett stability factor and condition of feedback oscillator design. *Proceedings of 8th International Conference on Telecommunications in Modern Satellite, Cable and Broadcasting Services (TELSIKS 2007)*, pp. 639-640.
18. Vishwakarma, S., Jung, S. & Joo, Y. J. (2004). Ultra wideband CMOS low noise amplifier with active input matching. *Proceedings of Joint Conference on Ultra wideband Systems and Technologies. (UWBST) & International Workshop on Ultra Wideband Systems (IWUWBS)*, pp. 415-419.